

Interaction induced phase transition in quantum many-body detection probability

Archak Purkayastha^{1,2,*} and Alberto Imparato^{3,†}

¹*Department of Physics, Indian Institute of Technology, Hyderabad 502284, India*

²*Centre for complex quantum systems, Aarhus University, Nordre Ringgade 1, 8000 Aarhus C, Denmark*

³*Department of Physics and Astronomy, Aarhus University,
Ny Munkegade, Building 1520, DK-8000 Aarhus C, Denmark*

(Dated: June 5, 2023)

We introduce and explore the physics of quantum many-body detection probability (QMBDP). Imagine a quantum many-body system starting from a far-from-equilibrium initial state. Few detectors are put at some given positions of the system. The detectors make simultaneous stroboscopic projective measurements of some chosen local operators. A particular measurement outcome is taken as the ‘signal’. By QMBDP we refer to the probability that the signal is detected within a given time. We find that, due to repeated stroboscopic measurements, there can emerge a time-scale within which the signal is almost certainly detected. Depending on the spectral properties of the Hamiltonian, there can be a phase transition where this time-scale increases dramatically on tuning some Hamiltonian parameters across the transition point. Consequently, over a finite but large regime of time, depending on the initial state, tuning some Hamiltonian parameters can result in sharp transition from a phase where the signal is certainly detected (QMBDP = 1) to a phase where the signal may not be detected (QMBDP < 1). As an example, we present a single-impurity non-integrable model where such a far-from-equilibrium transition is achieved by varying the many-body interaction strength.

Introduction— A fundamental question relevant across various branches of science is whether a chosen type of signal can be detected at a given position. One of the oldest mathematical formulations of the problem concerns a particle undergoing random walk. The seminal Pólya’s theorem [1] states that in one and two dimensions, the particle will be eventually detected with certainty regardless of the position of the detector, while in three dimensions there is a finite chance that the particle is never detected. In this work, we introduce and explore a quantum many-body version of the problem.

We consider a quantum many-body system starting from some far-from-equilibrium initial state, and imagine that detectors are put at some given positions of the system to detect a chosen signal. The chosen signal corresponds to a particular measurement outcome of simultaneous stroboscopic projective measurements by the detectors. By quantum many-body detection probability (QMBDP), we refer to the probability that the signal is detected within a given time. We show that, depending on the initial state, over a finite but large regime of time, tuning Hamiltonian parameters can lead to a sharp transition from a phase where the signal is certainly detected (QMBDP = 1), to a phase where the signal may not be detected (QMBDP < 1). Choosing a single-impurity non-integrable model, we demonstrate that such a phase transition can also be induced by tuning the strength of many-body interaction.

Although there have been few works exploring single-particle versions of the problem with single detectors [2–5], neither the effect of quantum many-body interactions,

nor detection based on simultaneous stroboscopic measurements at multiple positions, has been previously considered. In our example, it is the combination of both of these that leads to the transition in QMBDP. It is also worth mentioning that this far-from-equilibrium transition is not a class of measurement induced phase transition [6–9]. Instead, as we show, this transition is related with opening a specific type of gap in the many-body spectrum of the system. It can also manifest in far-from-equilibrium dynamical properties in absence of the detectors as we find in our example. However, we find that, at numerically accessible finite system-sizes, the transition in QMBDP is much sharper than that in other dynamical properties. Overall, our work initiates an exciting avenue for fundamental research at the interface of quantum many-body physics, quantum measurements and statistical physics, with potential implications for quantum technology.

QMBDP— Consider a quantum many-body lattice system with Hilbert space dimension D in a state far-from-equilibrium. Suppose that some detectors are placed at some specific sites, which are switched on in stroboscopic steps of time τ . The detectors make instantaneous projective measurement of some observable, say particle number, in those sites. In this situation, one can ask about the probabilities of making a chosen type of observation. For example, if there are two particle detectors, one can ask, what is the probability that they click simultaneously. We can think of the chosen type of observation as the ‘signal’. Let the Hamiltonian for the lattice system be \hat{H} , the initial state be $\hat{\rho}(0)$, the projection operator corresponding to measurement of the ‘signal’ be \hat{P} , and the complementary projection operator be $\hat{Q} = \hat{\mathbb{I}} - \hat{P}$, where $\hat{\mathbb{I}}$ is the identity operator. Using Born rule, the probability of not detecting the signal in n steps

* archak.p@phy.iith.ac.in

† imparato@phys.au.dk

is $R_n = \text{Tr}(\hat{M}^n(\tau)\hat{\rho}(0)\hat{M}^\dagger{}^n(\tau))$, $\hat{M}(\tau) = \hat{Q}e^{-i\hat{H}\tau}$. We call this no-detection probability. This is the analog of ‘survival probability’ studied in classical stochastic systems. The QMBDP, i.e, the probability that the signal is detected within time $n\tau$, is given by $T_n = 1 - R_n$. With a little algebra, the n th power of \hat{M} can be written as $\hat{M}^n(\tau) = \hat{M}_Q^{n-1}(\tau) \left(\hat{Q}e^{-i\hat{H}\tau}\hat{P} + \hat{M}_Q(\tau) \right)$, where

$$\hat{M}_Q(\tau) = \hat{Q}e^{-i\hat{H}\tau}\hat{Q}. \quad (1)$$

This is nothing but the projection of the unitary for time evolution onto the \hat{Q} subspace, i.e, the subspace where eigenvalue of \hat{Q} is 1. The physics of QMBDP is governed by spectral properties of $\hat{M}_Q(\tau)$.

The no-detection probability R_n is bounded from above by 1. So, the spectral radius of $\hat{M}_Q(\tau)$, i.e, the highest magnitude of its eigenvalues, must be ≤ 1 . Consequently, in complete generality, we can write the eigenvalues of $\hat{M}_Q(\tau)$ as $\{e^{-\lambda_m(\tau)+i\theta_m(\tau)}\}$, with $\lambda_m \geq 0$, θ_m being real, m going from 1 to D_Q , where $D_Q < D$ is the Hilbert space dimension of the \hat{Q} subspace.

Let the eigenvalues of $\hat{M}_Q(\tau)$ be arranged in ascending order of $\lambda_m(\tau)$. Then, we immediately see that for $\lambda_1(\tau) > 0$, i.e, when spectral radius is smaller than unity, if $n \gg 1/\lambda_1(\tau)$, the signal is almost certainly detected, irrespective of the initial state. Thus, $\tau/\lambda_1(\tau)$ gives the time scale for certainly detecting the signal. It is crucial to note that, this finite time scale for certainly detecting the signal irrespective of the initial state arises due to repeated stroboscopic measurements, and has no analog in absence of such measurements.

An interesting case arises if \hat{M}_Q has unit spectral radius, i.e, $\lambda_1(\tau) = 0$. In this case, depending on whether the initial state has substantial overlap with the corresponding eigenvector of $\hat{M}_Q(\tau)$, there is a finite probability that the signal is never detected. We now investigate how this situation can arise.

Condition for unit spectral radius of $\hat{M}_Q(\tau)$ for any finite τ — We prove that the necessary and sufficient condition for unit spectral radius of $\hat{M}_Q(\tau)$ at any finite value of τ is that some eigenvectors of \hat{H} belong entirely to the \hat{Q} subspace, i.e, are simultaneous eigenvectors of \hat{Q} with eigenvalue 1. Let the number of such eigenvectors be D'_Q , $D'_Q \leq D_Q$, and the projection operator onto this subspace be \hat{Q}' . Then, \hat{H} can be block-diagonalized as

$$\hat{H} = \hat{Q}'\hat{H}\hat{Q}' + \hat{P}'\hat{H}\hat{P}', \quad \hat{P}' = \hat{\mathbb{I}} - \hat{Q}'. \quad (2)$$

If the initial state belongs to \hat{Q}' subspace, the Hamiltonian dynamics does not take it outside of this subspace, and hence the signal will never be detected. This is irrespective of the value of τ . Consequently, depending on how much overlap the initial state has with \hat{Q}' subspace, there can be a finite probability of never detecting the signal. Thus, the sufficient direction of the proof is evident. The necessary direction is shown in the Appendix 1.

While the above results are general, in practice it can be difficult to check if \hat{H} satisfies Eq.(2), because full diagonalization of \hat{H} can be challenging. In the following, we give a perturbative way to find if this condition is approximately satisfied, based on spectral properties of a simpler Hamiltonian.

Relation with spectral gaps of Hamiltonian— Let $\hat{H} = \hat{H}_0 + \hat{H}_1$, where \hat{H}_0 is a simpler Hamiltonian, whose spectral properties are easily accessible, and \hat{H}_1 acts as a ‘perturbation’ on it. In particular, we consider a situation where, D_{Q_0} number of eigenvectors of \hat{H}_0 are known to completely belong to \hat{Q} subspace, with $D_{Q_0} \leq D_Q$. Let \hat{Q}_0 be the projection operator for this subspace. We have the block-diagonal structure $\hat{H}_0 = \hat{Q}_0\hat{H}_0\hat{Q}_0 + \hat{P}_0\hat{H}_0\hat{P}_0$, $\hat{P}_0 = \hat{\mathbb{I}} - \hat{Q}_0$. The Hamiltonian \hat{H}_1 mixes the two subspaces, but has no component completely within the \hat{Q}_0 subspace. The question is, with above assumptions, under what condition can a similar block-diagonalization be approximately preserved in presence of \hat{H}_1 .

The answer is succinctly provided by van Vleck perturbation theory. Let $|E_\alpha^{Q_0}\rangle$ be the eigenstate of \hat{H}_0 in \hat{Q}_0 subspace with energy $E_\alpha^{Q_0}$, while $|E_\nu^{P_0}\rangle$ be the eigenstate of \hat{H}_0 in \hat{P}_0 subspace with energy $E_\nu^{P_0}$. The Eq.(2) is approximately satisfied if for some range of $\alpha \in \{\alpha_{min}, \alpha_{max}\}$ the eigenstates of \hat{H}_0 in \hat{Q}_0 subspace are energetically gapped from those of \hat{P}_0 subspace in the sense

$$g_\alpha := \max_\nu \left| \frac{\langle E_\alpha^{Q_0} | \hat{H}_1 | E_\nu^{P_0} \rangle}{E_\alpha^{Q_0} - E_\nu^{P_0}} \right| \ll 1, \quad \alpha \in \{\alpha_{min}, \alpha_{max}\}. \quad (3)$$

Let the number of such eigenstates be $D'_Q \leq D_{Q_0}$, and \hat{Q}' be the projection operator onto this subspace. Under such conditions, starting with \hat{H} written in eigenbasis of \hat{H}_0 , van Vleck perturbation theory gives a systematic way to perturbatively find a unitary operator \hat{U}_r to r th order such that $\hat{U}_r^\dagger \hat{H} \hat{U}_r = \hat{H}^{(r)}$ is approximately block diagonal, i.e, $\hat{H}^{(r)} \simeq \hat{Q}'\hat{H}^{(r)}\hat{Q}' + \hat{P}'\hat{H}^{(r)}\hat{P}'$, with $\hat{P}' = \hat{\mathbb{I}} - \hat{Q}'$ [10, 11]. On further diagonalizing $\hat{H}^{(r)}$ the two subspaces mix only little. It follows that, Eq.(2) is satisfied to a good approximation.

Phase transition in detection probability— Suppose we have a situation where on changing a parameter in \hat{H}_0 across some value, an energy gap opens between some eigenstates in \hat{Q}_0 subspace and those of \hat{P}_0 subspace in the sense of Eq.(3). It is now clear that this will lead to a sharp decrease in $\lambda_1(\tau)$. So, we will have a transition from a phase with finite $\lambda_1(\tau)$ to a phase with $\lambda_1(\tau) \approx 0$. In terms of the non-unitary matrix \hat{M}_Q , this change in $\lambda_1(\tau)$ is reminiscent of gap closing in a quantum phase transition. Physically, the transition is from a phase where the signal is certainly detected in a finite time irrespective of initial state (QMBDP = 1), to a phase where, depending on the initial state, it may not be detected (QMBDP < 1). In the following, we discuss an illustrative example, where such a transition occurs

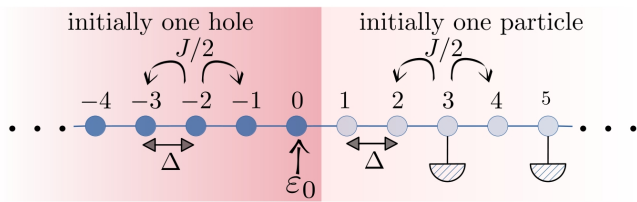


FIG. 1. The set-up consists of one-dimensional spinless fermionic lattice with nearest neighbour hopping strength $J/2$ and nearest neighbour many-body interaction Δ . There is an integrability-breaking on-site potential ε_0 only at site zero. $\hat{H} = -\sum_{\ell=-N/2+1}^{N/2-1} \left[\frac{J}{2} (\hat{c}_\ell^\dagger \hat{c}_{\ell+1} + \hat{c}_{\ell+1}^\dagger \hat{c}_\ell) + \Delta \hat{n}_\ell \hat{n}_{\ell+1} \right] + \varepsilon_0 \hat{n}_0$, where \hat{c}_ℓ is the fermionic annihilation operator at site ℓ and $\hat{n}_\ell = \hat{c}_\ell^\dagger \hat{c}_\ell$. Initially the left half has only one hole, while the right site has only one particle. Two detectors are placed making simultaneous stroboscopic projective measurements of particle numbers at sites p and q (here $p = 3$, $q = 5$) in intervals of time τ . The ‘signal’ is simultaneous detection on both detectors, the projection operator being $\hat{P} = \hat{n}_p \hat{n}_q$.

on tuning the strength of many-body interaction.

Model Hamiltonian— We consider the model Hamiltonian described and schematically shown in Fig. 1. With $\varepsilon_0 = 0$, this Hamiltonian can be Jordan-Wigner transformed into the integrable XXZ qubit chain. With $\varepsilon_0 > 0$, the model becomes the non-integrable single impurity XXZ chain [12–14]. This model has been of interest recently because despite being non-integrable, it inherits the ballistic transport of the integrable XXZ chain for $\Delta < J$ at high temperatures [14, 15]. However, the low temperature properties of the model are not well-explored to our knowledge.

Choice of signal— We divide the chain into left and right halves, the left half consisting sites $-N/2 + 1$ to 0, and the right half consisting of the remaining sites. We consider the case where, initially, there is only one hole (i.e, there are $N/2 - 1$ particles) on the left half of the chain, while there is only one particle on the right half of the chain (see Fig. 1). Note that this does not correspond to a single configuration. The exact form of initial state will be discussed later. We put two detectors on the right half, at sites p and q , $p, q > 0$, at a finite distance from the middle. They make simultaneous projective measurements of particle number in intervals of τ . We take simultaneous detection at the two sites as our signal. The corresponding projection operator is $\hat{P} = \hat{n}_p \hat{n}_q$, so $\hat{Q} = \hat{\mathbb{I}} - \hat{n}_p \hat{n}_q$. In the following we choose $p = 3$ and $q = 5$.

Choice of \hat{H}_0 , \hat{H}_1 and initial state— We choose $\hat{H}_1 = -\frac{J}{2} (\hat{c}_1^\dagger \hat{c}_0 + \hat{c}_0^\dagger \hat{c}_1)$, i.e, just the hopping term between left and right halves. Then $\hat{H}_0 = \hat{H} - \hat{H}_1$ is the Hamiltonian without this hopping term. Without this hopping, the number of particles in the left (N_L) and the right (N_R) halves are separately conserved. Let us restrict to the half-filling case, $N_L + N_R = N/2$, so that N_R is the only remaining quantum number. We immediately see that

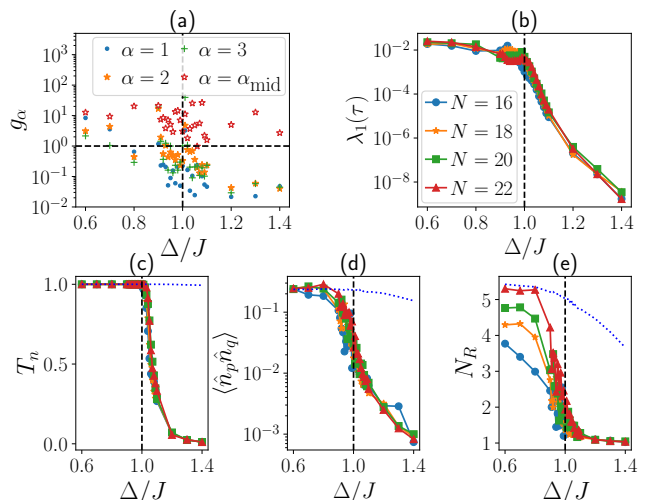


FIG. 2. (a) Plot of g_α (see Eq.(3)) with Δ for various values of α . Here $\alpha_{\text{mid}} = \lceil D_{Q_0}/2 \rceil$, and $N = 22$. (b) Plot of $\lambda_1(\tau)$ with Δ , for various system sizes. We choose $\tau = 2J^{-1}$. (c) Plot of detection probability, $T_n = 1 - R_n$, with Δ after $n = 1000$ steps, for the same system sizes. (d) Plot of $\langle \hat{n}_p \hat{n}_q \rangle$ with Δ at time $n\tau = 2000J^{-1}$, in absence of any detector, for the same system sizes. Here $p = 3$, $q = 5$. (e) Plot of N_R with Δ at time $n\tau = 2000J^{-1}$ in absence of any detector, for the same system sizes. For the continuous lines in (c), (d), (e) the initial state is of the form in Eq.(4) with $E = E_1^{Q_0}$, and the legend is the same as in (b). The dotted lines in (c), (d), (e) are the corresponding plots starting from a different initial state with $E = E_{\alpha_{\text{mid}}}^{Q_0}$, and system size $N = 22$. Other parameters, $\varepsilon_0 = 0.5J$, $\sigma = 0.1J$.

our choice of initial condition belongs to $N_R = 1$ sector of \hat{H}_0 . We take the initial state as an energy filtered random state in this sector of \hat{H}_0

$$|\psi(0)\rangle \propto \exp \left[- \left(\frac{\hat{H}_0 - E}{\sigma} \right)^2 \right] |\psi_{\text{rand}}\rangle_{N_R=1}, \quad (4)$$

where the $|\psi_{\text{rand}}\rangle_{N_R=1}$ is a randomly chosen state in $N_R = 1$ sector, and the prefactor is a Gaussian filter peaked around energy E with a standard deviation σ .

Since our ‘signal’ is detecting two particles simultaneously in the right half, the sectors with $N_R = 0, 1$ belong entirely to the \hat{Q} subspace. We define \hat{Q}_0 as the projector onto $N_R = 0, 1$ sectors. Our choice of initial state belongs to the Q_0 subspace. It is also clear that \hat{H}_1 connects N_R and $N_R + 1$ sectors. Therefore, to evaluate Eq.(3), we only need to diagonalize \hat{H}_0 in $N_R = 1$ and $N_R = 2$ subspaces. The Hilbert space dimensions of $N_R = 1$ and $N_R = 2$ subspaces of \hat{H}_0 scale as N^2 and N^4 respectively, which are far smaller than than exponential scaling of the Hilbert space dimension of the full \hat{H} in the half-filling sector.

Numerical techniques— The above simplification lets us find possible transition points in QMBDP. But it does not help in directly obtaining $T_n = 1 - R_n$. This is achieved as follows.

For pure initial state belonging to \hat{Q} subspace, $R_n = |\langle \psi_{R_n} | \psi_{R_n} \rangle|^2$, $\psi_{R_n} = \hat{M}_Q^n(\tau) |\psi(0)\rangle$. Since \hat{Q} is a strictly local operator, its operation on the state vector is simple. For time-evolution of a state vector with Hamiltonian, we use Chebyshev expansion [16–19] and carry out required matrix-vector multiplications using sparse representation of \hat{H} . This allows us to operate $\hat{M}_Q(\tau)$ on the state. Repeated operations of $\hat{M}_Q(\tau)$ yield R_n . Combining this with Arnoldi procedure [20, 21], we estimate the largest magnitude eigenvalue of $\hat{M}_Q(\tau)$, and thereby $\lambda_1(\tau)$. However, due to exponentially growing Hilbert space dimension, our results are limited up to system size $N = 22$ (Hilbert space dimension $D = 705432$). Despite this, we will see there is not much finite size effect, and the results are completely consistent with our analytical understanding.

Numerical results— In Fig. 2(a), we plot g_α as a function of Δ , for various values of α . We have arranged the eigenstates in \hat{Q}_0 subspace such that $\alpha = 0$ corresponds to $N_R = 0$, which is just one configuration, and $\alpha \geq 1$ are the eigenstates in $N_R = 1$ sector in ascending order of energy. In Fig. 2(a), we see that for the lowest few eigenstates in $N_R = 1$ sector, $g_\alpha \ll 1$ when $\Delta > J$, while this is not the case for $\Delta < J$. Contrarily, for a mid spectrum state, $\alpha = \alpha_{\text{mid}} = \lceil D_{Q_0}/2 \rceil$, we find $g_\alpha > 1 \forall \Delta$. Thus, we see clear evidence that Eq.(3) is satisfied in a low energy range when $\Delta > J$, while for $\Delta < J$, it is not satisfied. Consequently, we expect $\lambda_1(\tau)$ to drastically decrease on tuning Δ across 1. Indeed, this is clearly seen in Fig. 2(b), where we plot $\lambda_1(\tau)$ with Δ for $\tau = 2$.

It is interesting to note that, although our analysis is based on van Vleck perturbation theory, there is no obvious perturbative parameter in the system Hamiltonian. The Hamiltonian parameters, J , Δ and ε_0 are of same order. Regardless, with our choice of \hat{H}_1 , in a low-energy regime, a perturbative parameter emerges in the sense of Eq.(3), and governs the physics of quantum many-body detection probability.

Remember that the signal is almost certainly detected in $n \gg [\lambda_1(\tau)]^{-1}$ steps. So above results then suggest that, if we start from an initial state of the form of Eq.(4) with $E = E_1^{Q_0}$, and fix the number of steps n to be in the range $10^2 \ll n \ll 10^4$, which is finite but large, we should see a phase transition from $T_n = 1$ to $T_n < 1$ tuning Δ across 1. This is shown in Fig. 2(c), for $n = 1000$. The detection probability shows a clear sharp transition at $\Delta = J$.

One might naively think that this transition is occurring because high-temperature transport slows down on going across $\Delta = J$, and therefore particles from the left half cannot reach the sites p and q . However, this is not the case, because the sites $p = 3$ and $q = 5$ are at a finite distance from the middle and the time $n\tau = 2000J^{-1}$ is quite large. This is confirmed by the fact that if we start from an initial state with $E = E_{\alpha_{\text{mid}}}^{Q_0}$, we do not see any transition. Instead, in that case, we find that $T_n = 1$ for all Δ , as shown in Fig. 2(c) with dotted line. This is completely consistent with van Vleck perturbation the-

ory because mid-spectrum states do not satisfy Eq.(3), as shown in Fig. 2(a).

In Fig. 2(d), we show plots of the expectation value $\langle \hat{n}_p \hat{n}_q \rangle$ at time $n\tau$ in absence of any detectors, i.e, for continuous time evolution with the system Hamiltonian. This expectation value gives the probability of simultaneously detecting particles at sites p and q if a single projective measurement was done at time $n\tau$. We see that even for $\Delta < J$, $\langle \hat{n}_p \hat{n}_q \rangle \ll 1$. This clearly demonstrates that the unit detection probability for $\Delta < J$ observed previously in Fig. 2(c) is a consequence of multiple stroboscopic measurements. Nevertheless, we see that, when starting from initial state with $E = E_1^{Q_0}$, $\langle \hat{n}_p \hat{n}_q \rangle$ decreases fast on tuning Δ across 1. But, unlike for T_n , the decrease is far less sharp, and the transition point is not clear for this range of system sizes. We also see that, completely consistently, when starting from initial state with $E = E_{\alpha_{\text{mid}}}^{Q_0}$, there is no hint of any transition.

In Fig. 2(e), we show plots of the number of particles on the right half, N_R , at time $n\tau$ in absence of any detectors, i.e, for continuous time evolution with the system Hamiltonian. We find that, for $\Delta < J$, $N_R \sim N/4$. Thus, after this long time of evolution, the particles are approximately evenly distributed in the left and right halves of the chain, as would be expected in any generic system. However, when starting from initial state with $E = E_1^{Q_0}$, for $\Delta > J$, we see that N_R is close to 1. Thus, there has hardly been any transfer of particle to the right half. This is again completely consistent with the fact that since the initial state is in \hat{Q}_0 subspace, and Eq.(3) is satisfied for the low energy states, the dynamics hardly takes the system out of this subspace. So, we see a transition in N_R on changing Δ . However, at the numerically accessible system sizes, even this transition is not as sharp as that in T_n . Nevertheless, this shows that the phase transition in QMBDP would be observed for simultaneous detection in any two pair of sites on the right half. Further, since the dynamics in absence of measurements is independent of the choice of τ , it ensures that similar phase transitions in QMBDP would occur for any finite value of τ . When starting from initial state with $E = E_{\alpha_{\text{mid}}}^{Q_0}$, we find that N_R decreases smoothly with Δ with no hint of any sharp transition.

Relation with domain-wall melting— On Jordan-Wigner transforming, our choice of initial state is akin to a domain wall in the sense that total magnetization of the left half ($\propto N_L - N/2$) is positive and that of the right half ($\propto N_R - N/2$) is negative. Above results show that, for $E = E_1^{Q_0}$, the difference in magnetization ($\propto N_L - N_R$) is approximately preserved up to long time when $\Delta > J$. Thus, within this time, the domain wall ‘does not melt’ in this case. However, if $E = E_{\alpha_{\text{mid}}}^{Q_0}$, for all values of Δ , the domain wall melts. This is interesting because in terms of magnetization of left and right halves, there is no difference between the two initial states.

To our knowledge, the physics of domain wall melting has been previously explored in the single-impurity

non-integrable system in only one work [22], although it has extensively studied for integrable XXZ chains [23–29]. Moreover, most works focus on perfect domain wall between all spins up and all spins down regions, where, if it does not melt, the dynamics is almost frozen. Here, however, even when domain wall does not melt, the dynamics is not frozen, but is rather restricted to the \hat{Q}_0 subspace. This can be easily checked, for example, by plotting local occupation number of any site as a function of time (see Appendix 2). Thus, our analysis reveals that the underlying factors governing QMBDP also governs a slightly generalized domain wall melting phenomenon in the single-impurity non-integrable XXZ chain.

Conclusions— In this work, we have introduced the concept of QMBDP and discussed how this quantity can show a far-from-equilibrium phase transition due to opening of special types of gaps in the many-body spectrum of the Hamiltonian. In our example, this transition is brought about on tuning the strength of many-body interaction. Although the example is one-dimensional for numerical tractability, our analytical results are completely general. Our results might be experimentally checked in digital and analog quantum simulation platforms. Future work involves exploring QMBDP for different types of signals, systems and geometries, and possible consequences for technological applications.

Acknowledgments— We are grateful to Klaus Mølmer and Eli Barkai for helpful discussions. A.P acknowledges funding from the Danish National Research Foundation through the Center of Excellence “CCQ” (Grant agreement no.: DNRF156). A.P acknowledges the Grendel supercomputing cluster at Aarhus University where many of the calculations were done. A.P also thanks Anupam Gupta at Indian Institute of Technology, Hyderabad, for giving access to his workstation where some of the calculations were carried out.

APPENDIX

1. Necessary condition for finite no-detection probability irrespective of τ

Let us define the unitary operator $\hat{U}_Q(\tau) = e^{-i\tau\hat{Q}\hat{H}\hat{Q}}$. This unitary operator is the exponential of the Hamiltonian projected to the \hat{Q} subspace. We have $\hat{Q}\hat{H}\hat{Q}|E_m^Q\rangle = E_m^Q|E_m^Q\rangle$, where E_m^Q is the m th eigenvalue of $\hat{Q}\hat{H}\hat{Q}$, and $|E_m^Q\rangle$ is the corresponding eigenvector. The eigenvectors span the \hat{Q} subspace, and hence, $\hat{Q}|E_m^Q\rangle = |E_m^Q\rangle$. The eigenvalues of $\hat{Q}\hat{U}_Q(\tau)\hat{Q}$ are $\{e^{-i\tau E_m^Q}\}$, which have magnitude 1, and corresponding eigenvectors are $\{|E_m^Q\rangle\}$. The operator $\hat{M}_Q(\tau)$ can now be written as

$$\hat{M}_Q(\tau) = \hat{Q} \left[\hat{U}_Q(\tau) + \sum_{p=2}^{\infty} \frac{(-i)^p \tau^p}{p!} \left\{ \hat{H}^p - (\hat{Q}\hat{H}\hat{Q})^p \right\} \right] \hat{Q} \quad (5)$$

Let us assume τ is small, such that $\hat{M}_Q(\tau)$ can be treated as a perturbation over $\hat{Q}\hat{U}_Q(\tau)\hat{Q}$. Keeping only the leading order of the second term on right-hand-side in above equation, we have

$$\hat{M}_Q(\tau) \simeq \hat{Q}\hat{U}_Q(\tau)\hat{Q} - \frac{\tau^2}{2} \left(\hat{Q}\hat{H}^2\hat{Q} - \hat{Q}\hat{H}\hat{Q}\hat{H}\hat{Q} \right). \quad (6)$$

Assuming order by order expansion of eigenvalues and eigenvectors of $\hat{M}_Q(\tau)$ in τ , the leading order difference between eigenvalues of $\hat{M}_Q(\tau)$ and $\hat{Q}\hat{U}_Q(\tau)\hat{Q}$ is given by expectation value of the second term in above equation, in the eigenbasis of $\hat{Q}\hat{H}\hat{Q}$. This yields

$$e^{-\lambda_m(\tau) + i\theta_m(\tau)} \simeq e^{-i\tau E_m^Q} - \frac{\tau^2}{2} \left[\langle E_m^Q | \hat{H}^2 | E_m^Q \rangle - (E_m^Q)^2 \right]. \quad (7)$$

Taking logarithm of absolute value of above equation and keeping terms only up to the leading order in τ , we find the following insightful expression for $\lambda_m(\tau)$ to leading order in τ ,

$$\lambda_m(\tau) = \tau^2 \left[\langle E_m^Q | \hat{H}^2 | E_m^Q \rangle - (E_m^Q)^2 \right] + O(\tau^3). \quad (8)$$

This expression immediately shows that with $\tau \rightarrow 0$, $\lambda_m(\tau) \rightarrow 0$, $\forall m$. Thus, magnitude of all eigenvalues of $\hat{M}_Q(\tau)$ tend to 1 in this limit, meaning that the signal is never detected if the detectors are always kept on. This is the standard quantum Zeno effect.

Next, since $\lambda_m(\tau) \geq 0$, we have $\langle E_m^Q | \hat{H}^2 | E_m^Q \rangle - (E_m^Q)^2 \geq 0$. Consequently, for finite but small τ , the signal is always eventually detected, unless, for some choice of m , we have $\langle E_m^Q | \hat{H}^2 | E_m^Q \rangle - (E_m^Q)^2 = 0$. The later condition can only happen if $|E_m^Q\rangle$ is an eigenvector of \hat{H} with eigenvalue E_m^Q . Therefore, this eigenvector of \hat{H} must belong completely to the \hat{Q} subspace. However, if this is the case, by multiplying Eq.(5) with $|E_m^Q\rangle$ from right, we directly see that it is an eigenvector of \hat{M}_Q , the corresponding eigenvalue having $\lambda_m(\tau) = 0$ irrespective of the value of τ . Thus, some eigenvectors of \hat{H} belonging completely to the \hat{Q} subspace is a necessary condition for unit spectral radius of $\hat{M}_Q(\tau)$ for any finite value of τ .

2. Dynamics

Here we show the plots of dynamics of the system, in absence of any measurements, starting from the two different initial states corresponding to $E = E_1^{Q_0}$, $E = E_{\alpha_{\text{mid}}}^{Q_0}$. The plots are shown in Fig. 3.

In Fig. 3(a), when $E = E_1^{Q_0}$, we see that for $\Delta < J$, $N_R(t)$ (where we now explicitly write the time argument) increases with t towards $N_R(t) \sim N/2$. For $\Delta > J$, $N_R(t)$ remains close to $N_R(t) \sim 1$, over the entire time range considered. When $E = E_{\alpha_{\text{mid}}}^{Q_0}$, $N_R(t)$ increases towards $N/2$ for all values of Δ , as shown in Fig. 3(b). So, in the

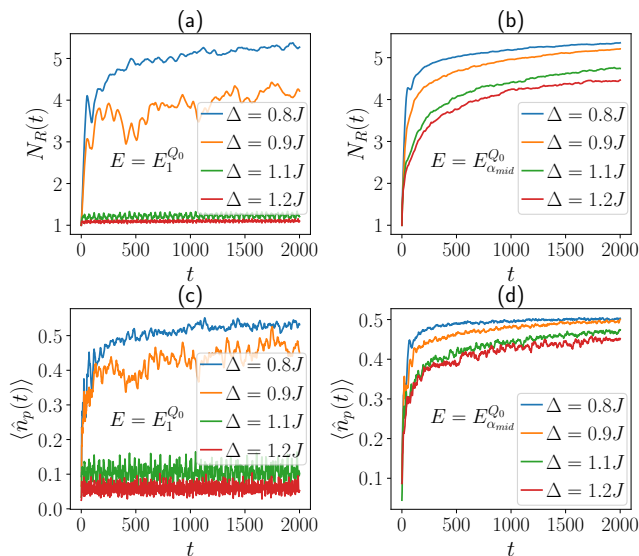


FIG. 3. (a) Dynamics of number of particles in right half, $N_R(t)$, for various values of Δ , when initial state is chosen with $E = E_1^{Q_0}$ in Eq.(4). (b) The same with $E = E_{\alpha_{mid}}^{Q_0}$. (c) Dynamics of occupation at site $p = 3$, for various values of Δ , when initial state is chosen with $E = E_1^{Q_0}$ in Eq.(4). (d) The same with $E = E_{\alpha_{mid}}^{Q_0}$. Other parameters, $N = 22$, $\epsilon_0 = 0.5J$, $\sigma = 0.1J$.

domain wall picture, we clearly see that the domain wall does not melt for $\Delta > J$, and $E = E_1^{Q_0}$, while in other cases, it melts, as expected in non-integrable systems.

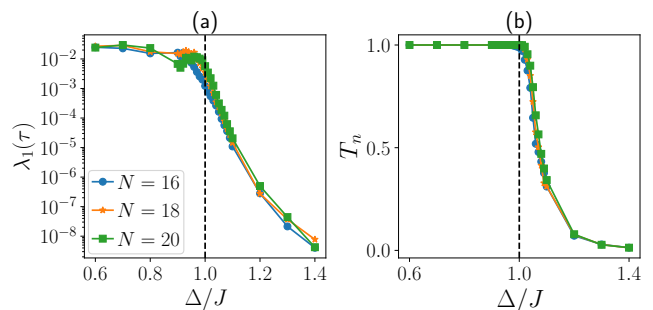


FIG. 4. a) Plot of $\lambda_1(\tau)$ with Δ , for various system sizes, and for $\tau = 4J^{-1}$. (c) Plot of detection probability, $T_n = 1 - R_n$, with Δ after $n = 1000$ steps, for the same system sizes, and for $\tau = 4J^{-1}$. Other parameters, $\epsilon_0 = 0.5J$, $\sigma = 0.1J$.

In Fig. 3(c), we plot the dynamics of occupation at site p , $\langle \hat{n}_p(t) \rangle$, with $p = 3$, for various values of Δ , starting with the initial state corresponding to $E = E_1^{Q_0}$. The occupation approaches $\langle \hat{n}_p(t) \rangle \sim 0.5$ for $\Delta < J$, which it shows oscillations about a much smaller value for $\Delta > J$. The important point to note here is that even for $\Delta > J$, where the domain wall does not melt, the dynamics is not completely frozen. Rather, it is restricted to a small subspace. In Fig. 3(d), we show similar plots starting with the initial state corresponding to $E = E_{\alpha_{mid}}^{Q_0}$. In this case, the occupation approaches $\langle \hat{n}_p(t) \rangle \sim 0.5$ for all values of Δ considered here.

3. Different choice of τ

Our analytical understanding shows that the phase transition in QMBDP is independent of the choice of τ . In Fig. 4 we show plots of $\lambda_1(\tau)$ versus Δ , and QMBDP $T_n = 1 - R_n$ for $n = 1000$, and $\tau = 4J^{-1}$. This value of τ is different from that of the plots in the main text, where $\tau = 2J^{-1}$. We still see precisely the same behavior phase transition in QMBDP.

-
- [1] G. Pólya, *Mathematische Annalen* **84**, 149 (1921).
 - [2] F. Thiel, I. Mualem, D. Kessler, and E. Barkai, *Entropy* **23** (2021), 10.3390/e23050595.
 - [3] F. Thiel, I. Mualem, D. Meidan, E. Barkai, and D. A. Kessler, *Phys. Rev. Res.* **2**, 043107 (2020).
 - [4] F. Thiel, I. Mualem, D. A. Kessler, and E. Barkai, *Phys. Rev. Res.* **2**, 023392 (2020).
 - [5] S. Dhar, S. Dasgupta, A. Dhar, and D. Sen, *Phys. Rev. A* **91**, 062115 (2015).
 - [6] M. Buchhold, Y. Minoguchi, A. Altland, and S. Diehl, *Phys. Rev. X* **11**, 041004 (2021).
 - [7] Q. Tang and W. Zhu, *Phys. Rev. Res.* **2**, 013022 (2020).
 - [8] B. Skinner, J. Ruhman, and A. Nahum, *Phys. Rev. X* **9**, 031009 (2019).
 - [9] S. Dhar and S. Dasgupta, *Phys. Rev. A* **93**, 050103 (2016).
 - [10] I. Shavitt and L. T. Redmon, *The Journal of Chemical Physics* **73**, 5711 (1980).
 - [11] C. Cohen-Tannoudji, J. Dupont-Roc, and G. Grynberg, *Atom-Photon Interactions: Basic Process and Applications* (WILEY-VCH Verlag GmbH and Co. KGaA, Weinheim, 2004).
 - [12] L. F. Santos, *Journal of Physics A: Mathematical and General* **37**, 4723 (2004).
 - [13] M. Brenes, T. LeBlond, J. Goold, and M. Rigol, *Phys. Rev. Lett.* **125**, 070605 (2020).
 - [14] M. Brenes, J. Goold, and M. Rigol, *Phys. Rev. B* **102**, 075127 (2020).
 - [15] M. Brenes, E. Mascarenhas, M. Rigol, and J. Goold, *Phys. Rev. B* **98**, 235128 (2018).
 - [16] H. Tal-Ezer and R. Kosloff, *The Journal of Chemical Physics* **81**, 3967 (1984).

- [17] R. Chen and H. Guo, *Computer Physics Communications* **119**, 19 (1999).
- [18] V. V. Dobrovitski and H. A. De Raedt, *Phys. Rev. E* **67**, 056702 (2003).
- [19] H. Fehske, J. Schleede, G. Schubert, G. Wellein, V. S. Filinov, and A. R. Bishop, *Physics Letters A* **373**, 2182 (2009).
- [20] W. E. Arnoldi, *Quarterly of Applied Mathematics* **9**, 17 (1951).
- [21] Z. xiao Jia and L. Elsner, *Journal of Computational Mathematics* **18**, 265 (2000).
- [22] L. F. Santos and A. Mitra, *Phys. Rev. E* **84**, 016206 (2011).
- [23] G. Misguich, N. Pavloff, and V. Pasquier, *SciPost Phys.* **7**, 025 (2019).
- [24] O. Gamayun, Y. Miao, and E. Ilievski, *Phys. Rev. B* **99**, 140301 (2019).
- [25] G. Misguich, K. Mallick, and P. L. Krapivsky, *Phys. Rev. B* **96**, 195151 (2017).
- [26] J.-M. Stéphan, **2017**, 103108 (2017).
- [27] J. Mossel and J.-S. Caux, *New Journal of Physics* **12**, 055028 (2010).
- [28] S. Yuan, H. De Raedt, and S. Miyashita, *Phys. Rev. B* **75**, 184305 (2007).
- [29] D. Gobert, C. Kollath, U. Schollwöck, and G. Schütz, *Phys. Rev. E* **71**, 036102 (2005).